JOURNAL OF MATERIALS SCIENCE 31 (1996) 655–662

A method of measuring energy dissipation during crack propagation in polymers with an instrumented ultramicrotome

M. L. ERICSON, H. LINDBERG*
*Division of Polymer Engineering, Luleå University of Technology, S-971 87, Luleå, Sweden and *Department of Wood Technology, SKERIA 3, Luleå University of Technology, S-931 87, Skellefteå, Sweden*

In order to characterize very local energy dissipation during crack propagation in polymers, an ultramicrotome was instrumented to measure the energy dissipated during sectioning. The work to section per unit area, W_S, was measured for five different amorphous polymers [polymethyl methacrylate (PMMA), polystyerene (PS), polycarbonate (PC) and two epoxy resins] in the glassy state. When the section thickness was varied between 60 and 250 nm, W_S varied between 15 and 100 Jm^{-2}, depending on the material and section thickness. The method and the results are compared with other methods used for determining the energy dissipation at a local level as well as at a macroscopic level in polymers. The differences between different polymers were found to be contradictory to macroscopic fracture toughness, G_{Ic}, measurements. The material that showed the highest W_S had the lowest G_{Ic} values reported. Possible mechanisms for energy dissipation during sectioning are also discussed.

1. Introduction

The energy required to extend a crack over a unit area in a solid is often termed the fracture energy or the critical strain energy release rate, G_c. In the case of amorphous polymers, G_c depends generally on molecular weight (or the molecular weight between crosslinks, M_c), molecular orientation, crack velocity, temperature and the applied strain [1]. During crack propagation in amorphous polymers several energy dissipation mechanisms may contribute to G_c, from chain scission at the fracture plain to large scale plastic deformation at the crack tip. If the temperature is above the glass transition temperature, T_g, large scale molecular motions may cause extensive plastic deformation at the crack tip. G_c is then high and extremely time and temperature dependent. King and Andrews [2] showed that G_c for an epoxy obeys the Williams-Landel-Fery (WLF) time–temperature superposition at temperatures above T_g.

However, at temperatures below T_g the relaxation time for large scale molecular motion is longer than the time scale of the experiment. Therefore, other energy dissipation mechanisms than described above may then dominate. Such mechanisms include chain scission and cleavage of secondary bonds, and the development of subcrack systems.

The level of G_c depends on the active mechanisms and the activation volume. The theoretical minimum for G_c is termed the intrinsic fracture energy, G_0, and represents the energy to cleave secondary and primary bonds at the fracture surface. G_0 is independent of time and temperature. G_c may then be described as

$$G_c = G_0 + \psi \quad (1)$$

where ψ is the energy dissipated in mechanisms such as viscoelastic and plastic deformation [1] and the development of subcrack systems.

If only secondary bonds were ruptured in a polymer, then $G_c = G_0 = 2\gamma$, where γ is the surface free energy, typically 0.04 Jm^{-2} (see Table I). However, crack propagation in polymers also necessitates rupture of stronger covalent bonds. Typical levels of G_0 at the order of 1 Jm^{-2} have been reported (see Table I) [1, 5]. When measuring G_c by macroscopic tests, such as compact tension (CT) or double cantilever beam (DCB), considerable higher values of G_{Ic} (index I for crack opening mode) are found, typically 500–1000 Jm^{-2}. The reason is that even for the most brittle polymers, crack propagation is dominated by other mechanisms than pure chain scission at the crack plane. Methods of increasing the volume of activated material have been the focus of a large body of research since the early 1970s.

In order to understand the rule of different energy dissipation mechanisms one needs methods to quantify the dissipated energy on all levels, the molecular level and the macroscopic level. To the authors' knowledge, only a small number of methods for the measurement of dissipated energy at a very local level have been reported. Many methods include the propagation of a more or less known crack through the material [2, 11, 13–14], but methods based on

0022–2461

TABLE I Properties of the five amorphous polymers studied

Material	Surface free energy[a], γ ($J m^{-2}$)	Intrinsic fracture energy[b], G_0 ($J m^{-2}$)	Fracture energy at 20 °C[c], G_{Ic} ($J m^{-2}$)	Young's modulus[d], E (GPa)	Glass transition temperature[e], T_g (°C)
DGEBA/DETA	–	–	130	2.1	107
DGEBA/APTA	–	–	300	2.4–3.2	93
PS	0.040–0.041	0.5	300–400	3.2–3.4	95
PC	0.042–0.043	0.6	1500	2.4	150
PMMA	0.039–0.041	0.4–0.5	500	3.3	105

[a] Data from [1, 3–5].
[b] Data from [1, 5].
[c] Data from [1, 6–8].
[d] Data from [4, 5, 9–11].
[e] Data from [10, 12].

grinding techniques have also been reported [15–18]. However, most methods include tedious experimental work and or indirect material characterization.

Fordyce *et al.* [17] accomplished mechanical degradation by grinding PS under liquid nitrogen using a dental burr in a handgrinder. The number of chain ruptures per square metre were determined by electron spin resonance spectroscopy (ESR), fourier transform infrared spectroscopy (FT–i.r.) and viscometry to be between 10^{17} and 10^{18}. This corresponds to a fracture energy about $1 J m^{-2}$. Mohammadi *et al.* [16] used a dental burr connected to a rheometer and measured the fracture energy and the molecular weight distribution before and after cutting in a PS latex film. Fracture energy depended on annealing time and the maximum energy measured was $2.5 J m^{-2}$. Yang *et al.* [18] used impact fragmentation by an air jet pulverization process and evaluated the number of chain scissions by measuring the molecular weight reduction and the total fracture area by size exclusion chromatography and statistical particle size measurements, respectively. The number of chain scissions was found to be $3.3 \times 10^{18} m^{-2}$ in PS. This corresponds to a fracture energy of about $1 J m^{-2}$.

In an attempt to measure G_0, Lake and Lindley [11] evaluated the fatigue limit for rubbers. By measuring the tearing energy and extrapolating data to zero crack velocity they measured G_0 to be the same order of magnitude as later modelled by Lake and Thomas [19] (about $50 J m^{-2}$). However, in order to lower the great scatter the experiment would need to be performed at extremely low crack speeds and is therefore tedious. King and Andrews [2] modified a theoretical model for highly cross-linked networks in the rubbery state. The fatigue method did not work well, but static loading tests gave good correspondence to model values. Depending on the epoxy resin tested, G_0 was found to vary between 3.8 and $5.7 J m^{-2}$.

Another attempt is presented by Vincent and coworkers [15, 20, 21]. Their idea is to use a microtome instrumented to measure cutting forces. When the thickness of the sections were decreased continuously from 1 mm to 1 μm the sectioning energy also decreased. Atkins and Vincent [15] suggested that the sectioning energy extrapolated to zero thickness is G_c. They used a rotary microtome fitted with a modified knife holder as a load cell. No measurements on polymers were recorded, but an interesting study on meat was published by Dobraszczyk *et al.* [22]. Wool and Rockhill [13] studied the molecular degradation during microtome sectioning by viscometry. Hodson and Marshall [23] and Saubermam *et al.* [24] presented alternative methods for evaluating the sectioning forces on a microtome.

The idea of controlling the studied volume during crack propagation by sectioning could further be refined to ultramicrotome sectioning. Wikefeldt [25] reported fracture energies as low as $16 J m^{-2}$ for PMMA. Unfortunately these results were only presented in a PhD thesis (in Swedish) and were not discussed in terms of G_c and G_0. Helander [26] also measured forces during ultramicrotome sectioning for varying epoxy sectioning conditions. However, he only reported forces (mN) and did not give results in terms of work to section. Willett *et al.* [27] sectioned PS rods with an ultramicrotome and concluded that around 7×10^{17} chain scissions per square metre took place.

Several techniques to determine the sectioning forces during ultramicrotome sectioning have been reported [23, 25–27]. Wikefeldt [25] placed two piezoelectric elements in the drive arm of the ultramicrotome. Then it was possible to measure both forces acting perpendicular and parallel to the sectioning direction. Hodson and Marshall [23] calculated the forces acting on the substrate by measuring the velocity of the specimen arm by an electromagnetic induction method. When they knew the mass and the retardation it was possible to calculate the sectioning forces.

Apart from the interest of a more complete understanding of fracture mechanisms, deeper insight of the ultramicrotome cutting could be used in order to optimize cutting techniques in the quest for perfect, or at least reproducible, sections for quantitative studies.

The objective of this study is to evaluate the possibility of using an instrumented ultramicrotome to measure energy dissipation during sectioning of polymers. Five amorphous polymers in the glassy state are sectioned with varying section thickness. The method and the results are compared with other methods used

for determining the energy dissipation at a local level, as well as at a macroscopic level, in polymers. Furthermore, the results are also compared with theoretical values found in the literature, and the mechanisms for energy dissipation during sectioning is discussed.

2. Experimental procedure

2.1. Materials

Five amorphous polymers were studied, two epoxies Diglycidyl ether of bisphenol A/Diethyl triamine (DGEBA/DETA and Diglycidyl ether of bisphenol A/Polyoxy propyleneamine DGEBA/APTA) and three thermoplastics (PS, PMMA and PC), see Table II. Since the thermoplastics were cut from commercially available extruded sheets they are believed to have relatively high molecular weight.

2.2. Specimen preparation

The two epoxy systems were cast into sheets according to the suppliers recommendations and the thermoplastics were cut from extruded sheets of 2 mm. A fine hand saw was used to cut samples from the sheets for further preparation in the ultramicrotome. In order to obtain a controlled shape suitable for ultramicrotoming, the specimens were trimmed in the ultramicrotome with a glass knife to yield an appropriate sectioning area, a so called "mesa", of approximately 1 mm^2. The dimensions of the mesa were measured in an optical microscope with calibrated magnification.

2.3. Microtome cutting and thickness measurement

The ultramicrotome used in this study was an LKB Ultrotome V with a diamond knife. The ultramicrotome has a very accurate feed mechanism which gives good reproducibility of section thickness at the used setting. The thermal advance mechanism is accurate, especially below section thicknesses of 100 nm.

The cutting force is obtained by speed control of the falling weight of the specimen holder arm. The maximum force, which could be obtained, was approximately 3.4 N. Generally the cutting speed was set to 1 mm s^{-1}.

In Fig. 1 a schematic of the sectioning is presented. The diamond knife, which according to the manufacturer has an edge radius of 5–7 nm, is forced to section the mesa of 1 mm^2. When the edge of the knife is sectioning, a force will act on the substrate and the force transducer will respond accordingly. The force acting on the polymer sample could be separated into two perpendicular components. The force parallel to the sectioning direction is termed the tangential force, F_t, and the force perpendicular to the sectioning direction is termed the radial force, F_r.

The thickness of the cuts were determined from the interference colours created by the difference in path length between the rays reflected at the section surface and rays reflected at the water surface below. Table III shows the used thicknesses for read colours calculated after Patzelt [28].

TABLE II Materials used in the study

Material	Description
DGEBA/DETA	The epoxy system DGEBA (DER 332 from Dow Chemical Co.) and curing agent DETA (DEH 20 from Dow Chemical Co.). Mixing ration 100:11.9 by weight
DGEBA/APTA	The epoxy system DGEBA (DER 332 from Dow Chemical Co.) and curing agent APTA (Jeffamine T-403 from Texaco Chemical Co.). Mixing ration 100:44.8 by weight
PS	Polystyrene from extruded sheet
PC	Polycarbonate from extruded sheet
PMMA	Polymethyl methacrylate from extruded sheet

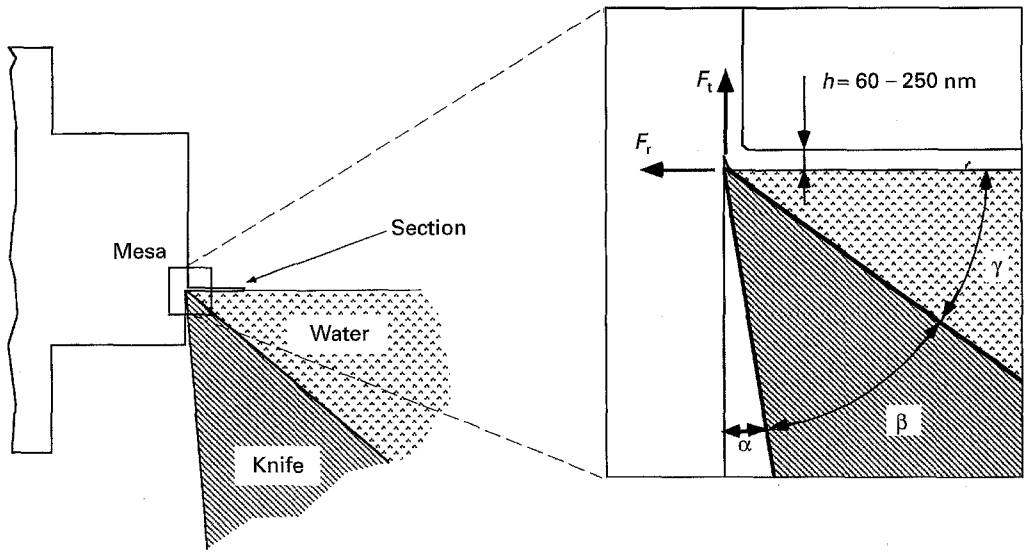

Figure 1 Schematic diagram of sectioning by an ultramicrotome α, clearance angle; β, bevel angle; γ rake angle.

TABLE III Interpretation of interference colour for two different refractive indices

Interference colour	Section thickness, h (nm)	
	$n = 1.5$[a]	$n = 1.6$[b]
Silver-grey	50–70	50–75
Silver	70–100	75–107
Gold	100–130	107–140
Violet	130–180	140–190
Blue	180–240	190–255

[a] PMMA
[b] Epoxy, PC, PS

2.4. Sectioning force measurements

In order to obtain the work to section, W_S, the sectioning forces, F_t and F_r in Fig. 1, acting on the polymer substrate (or on the diamond knife) are needed. For that purpose a special sample holder which enables force measurements was designed and built, see Fig. 2a, b. It is a construction in two halves, held together by a prestressed force transducer (load cell). In order to prevent mechanical vibrations, so called chatter, effort was made to make the instrumented sample holder as stiff as possible in the direction perpendicular to the sectioning direction. The quartz force transducer was a Kistler 9207 with a Kistler charge amplifier, type 5011 A11 (Kistler Instrumente AG). The signal from the amplifier was sampled by a computer for further data manipulation.

Since the sample holder was designed to detect mainly tangential forces, a special technique was developed to obtain the radial force, F_r. First, the sample was trimmed and prepared with the axis of the force transducer not parallel, but tilted at an angle $\phi = 10°$ towards the knife. The recorded forces are therefore a combination of both F_t and F_r. Since F_t is measured in a separate measurement, F_r can be calculated through

$$F_r = \frac{F_t(0°) \times \cos\phi - F_t(\phi)}{\sin\phi} \quad (2)$$

where F_t (0°) is the known tangential force for no tilting and F_t (ϕ) is the tangential force for tilting angle, ϕ.

2.5. Measurement of dimensional changes

It is widely known that, when sectioning with an ultramicrotome, the resulting sections are often compressed in the sectioning direction [26, 29]. In order to measure these dimensional changes the optical microscope mounted on the ultramicrotome was connected to a video camera and the magnification calibrated. A computer with an image analysis program recorded the width and length of the sections when they entered the water trough behind the edge of the knife. The sections were focused and measured just when they left the mesa. To obtain undeformed dimensions, the mesa was focused and measured. Dimensional changes were recorded for PMMA and DGEBA/DETA, on four and six sections, respectively. A compression factor, $r = l/l_i$, was calculated, where l is the length of the section and l_i the section length before sectioning (on the mesa).

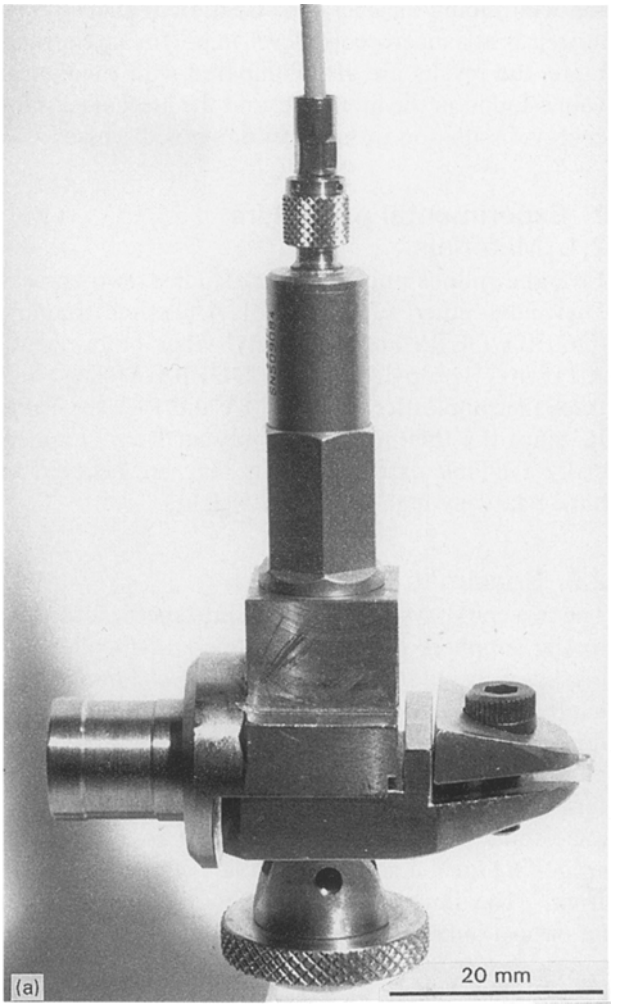

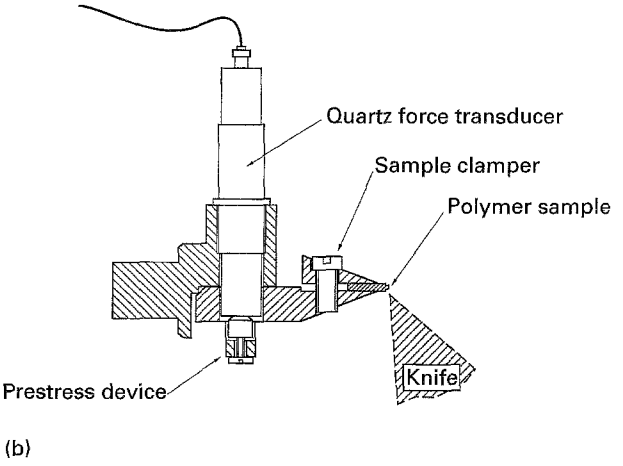

Figure 2 The instrumented sample holder for the ultramicrotome (a) photo, and (b) schematic diagram.

2.6. Calculation of the work to section

Since the radial sectioning force, F_r, does not do any mechanical work, only the tangential sectioning force, F_t, was used for the calculation of the total work to section, W_S. The work done per unit area in the

sectioning direction is

$$W_S = \frac{F_t}{b} \quad (3)$$

where b is the width of the sample mesa.

3. Results and discussion

3.1. Sectioning force measurements

The instrumented sample holder worked as expected in terms of sensitivity and function. An existing ultramicrotome can be used with modification of only the sample holder. Therefore the required investment is quite small. Results from the calibration, Fig. 3, show that the instrumented sample holder has a linear response, mainly on the tangential force component, and is very sensitive. Forces as low as 5 mN could be measured. In Fig. 3a the load cell response, F_L (the force changes detected by the piezoelectric force transducer), is plotted versus the substrate force, F_Θ. Data for two loading angles, tangential ($\Theta = 90°$) and radial ($\Theta = 180°$), and two levels of prestress in the load cell are presented in the graph. As found in Fig. 3a, the load cell response is linear with respect to F_Θ and is dominant in the tangential direction, 30 times stronger than the radial response. Another proof of the dominant tangential response is presented in Fig. 3b, where F_L as a function of Θ follow a sinusoidal function very close, see the dashed lines in Fig. 3b. A disadvantage is that the load cell response also depends on the level of load cell prestress, F_{L0}. As seen in Fig. 3a, a change in F_{L0} from 15 to 30 N decreases the response by approximately 15%. This makes it extremely important to keep constant F_{L0} throughout the experiment.

During the development of the instrumented sample holder one found that the stiffer the sample holder, the better section-to-section reproducibility. This was also pointed out by Atkins and Vincent [15]. Since all methods for force measurements need some displacement this demand contradicts the design possibilities. The compliance of the load cell used is $4 \cdot 10^{-6}$ nm mN^{-1} and seems to work well in the tangential direction.

Figs 4 and 5 show typical F_t outputs during sectioning. Remarkable section-to-section reproducibility of the force measurements during serial sectioning was found. An example of this is seen in Fig. 4 were F_t for PC with violet interference colour (section thickness, h, is between 140 and 190 nm) is plotted. A small decrease in F_t sometimes observed was found to be a drift. The thickness reproducibility of the used ultramicrotome at a given setting was found earlier [29] to be extremely good. All five materials showed the same remarkable reproducibility and the differences seen between individual curves are believed to be due to thickness variations below the resolution of the used interference method.

In Fig. 5 the tangential sectioning force, F_t, versus sectioning time for four different section thicknesses of PMMA is plotted. Although the cutting length is constant, the thicker sections usually take a longer

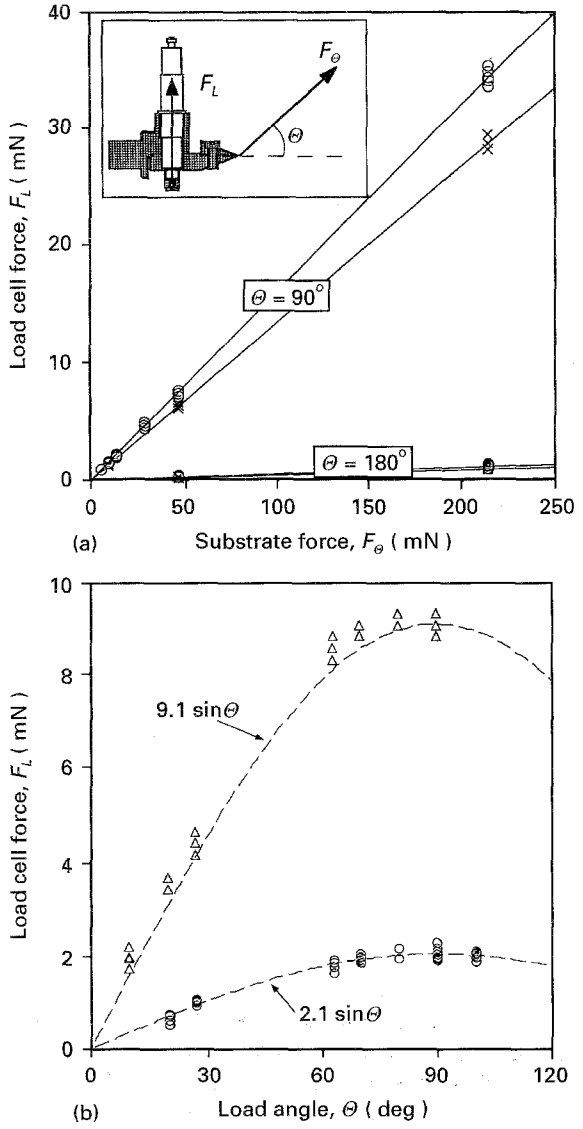

Figure 3 Calibration data for the instrumented sample holder (a) load cell force, F_L, versus substrate force, F_Θ for two loading angles and two levels of load cell prestress, F_{L0}: (○) 15 N, (×) 30 N; and (b) load cell force, F_L versus load angle, Θ, for two levels of substrate force, F_Θ: (△) 46 mN, (○) 9.7 mN.

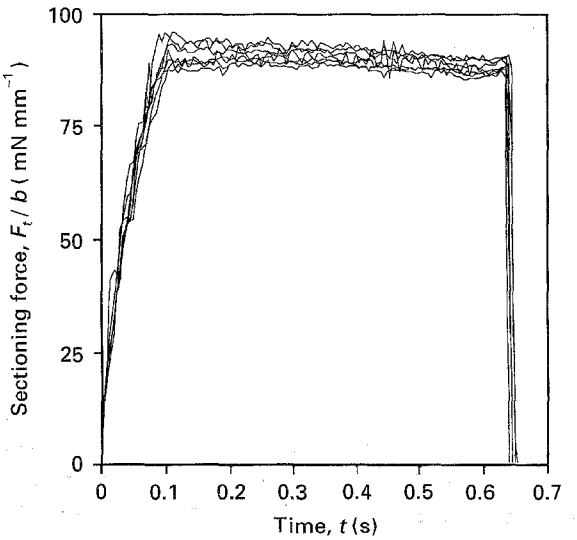

Figure 4 Typical curves of tangential sectioning force, F_t, versus time for PC. The interference colour of all sections was violet, (i.e. $h \approx 140$–190 nm).

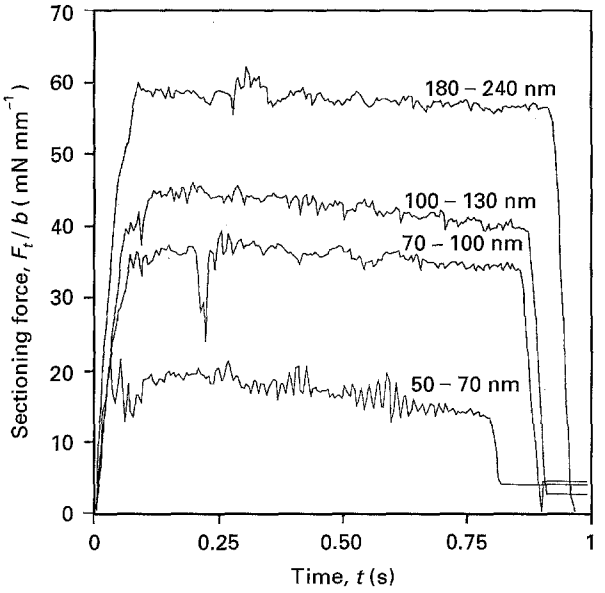

Figure 5 Typical curves of tangential sectioning force, F_t, versus time for different section thicknesses of PMMA.

TABLE IV Dimensional changes of sections of PMMA and DGEBA/DETA

Measurements	PMMA (four sections)	DGEBA/DETA (six sections)
Initial width, b_i, mm	0.82	0.95
Section width, b, mm	0.86	0.99
	0.86	0.98
	0.85	1.01
	0.85	0.98
		1.00
		1.00
Initial length, l_i, mm	0.69	1.22
Section length, l mm	0.65	1.11
	0.63	–
	0.64	1.05
	0.63	1.02
		1.07
		1.03
Average area change, %	– 2.1	– 9.4
Average compression factor, l/l_i	0.92	0.86

time to section. These minor changes in sectioning speed are disregarded in the further analysis.

Despite the remarkable section-to-section reproducibility, the instrumented sample holder showed quite poor sample-to-sample reproducibility. When changing a sample, by dismounting the sample holder, the load cell response could vary as much as ± 20%, even for identical materials and sectioning conditions. The reason for this unwanted effect is believed to be due to difficulties in mounting the two halves of the sample holder in exactly the same position as before. Also, different heating (e.g. due to contact with hands) of the sample holder when handling it during sample mounting could alter slightly the prestress, F_{LO}, resulting in an altered load cell response. Therefore it was of significant importance to minimize these effects by careful handling and sample mounting.

The large sample-to-sample variation is quite a severe problem when absolute measurements are to be performed. Nevertheless, one believes that this technique still is attractive since it is a direct method without other indirect characterization techniques. One also believes that it is possible to improve reproducibility by redesigning the sample holder. An alternative route is to perform relative measurements by sectioning several materials at the same time, with a hybrid sample built of a thin lamellae of each material.

The radial force, F_r, acting upon the sample was estimated by the procedure described above. However, due to poor sample-to-sample reproducibility, it was difficult to draw any conclusions. Data do, however, indicate that F_r is positive, i.e. the knife is pushed into the substrate, and larger than F_t. For a thorough understanding of the section process it is crucial to be able to measure F_r more accurately. Therefore redesigning the sample holder is an important step for future work. If the sample holder were stiffer, it may be possible to section an even thinner section than done here.

3.2. Dimensional changes of sections

Dimensional changes of the sections were measured for PMMA and DGEBA /DETA as described above. The results are presented in Table IV. As seen, the section length is shorter than the mesa, whereas the width is longer. The total area change was – 2.1 and – 9.4% for PMMA and DGEBA/DETA, respectively, and is dominated by the change in length. Therefore the compression factor, r, was chosen to characterize the dimensional changes. As seen in Table IV, r was approximately 0.92 for PMMA and 0.86 for DGEBA/DETA. Helander [26] observed similar values, between 0.71 and 0.93, for different epoxies at different sectioning conditions. If the volume of the sections is constant, the compression also results in thickening of the as-cut section.

3.3. Work to section

The work to section, W_S, for the five glassy amorphous polymers, as a function of section thickness, h, is presented in Fig. 6. As observed by Wikefeldt [25] for ultramicrotomy and Vincent and coworkers [15, 20, 21] for microtomy, W_S increases with h. The slopes in Fig. 6 differ between different polymers, but they seem to converge to similar very low values for small h. If the curves in Fig. 6 were extrapolated to smaller h, then W_S would be lower than 10 J m^{-2} for all tested materials. Both Wikefeldt [25] and Vincent and coworkers [15, 20, 21] assumed W_S versus h to be linear and therefore easily extrapolated down to $h = 0$. However, as seen Fig. 6, W_S is not necessarily linear. Especially, for the two thermosets (DGEBA/DETA and DGEBA/APTA) W_S increases stepwise for increasing h. It is therefore difficult to extrapolate to smaller (or larger) section thicknesses. Data for PMMA from Wikefeldt [25] are also presented in Fig. 6. Although he just used the ultramicrotome settings for the thickness the two experiments almost

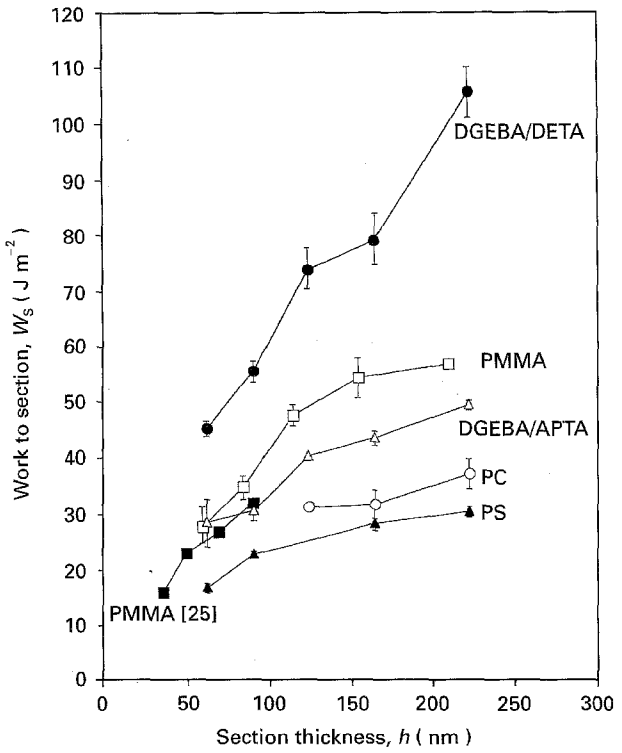

Figure 6 Work to section per unit area, W_S, versus section thickness, h, for the five studied polymers at ambient sectioning temperature. The error bars are the section-to-section standard deviation. The error in h is according to Table III.

overlap. This indicates that the type of PMMA tested is of minor significance at small h.

If one compares macroscopic G_{Ic} data, see Table I, with Fig. 6 it is clearly seen that order between the materials does not compare. The order in W_S between the materials is: DGEBA/DETA > PMMA > DGEBA/APTA > PC > PS. G_{Ic} values for the same order, are (see Table I): 130, 500, 300, 1500 and 300 J m^{-2} respectively. Despite the poor sample-to-sample reproducibility one concludes that DGEBA/DETA shows W_S significantly higher than the other four materials. It is interesting to find that PC, which has the highest macroscopic G_{Ic}, shows the lowest W_S, and vice versa for DGEBA/DETA. This indicates that the mechanisms for crack propagation differ significantly between ultramicrotomy and macroscopic fracture mechanic tests.

3.4. Mechanisms for energy dissipation

What mechanisms for energy dissipation could explain the measured W_S? It is believed that the work to cut just the primary and secondary bonds at the crack plane is in the order of 1 J m^{-2} [1, 5], regardless of the type of isotropic polymer. What other energy dissipation mechanisms could be active? Other possible mechanisms include: bending of the as-cut section, friction between the knife and the substrate, molecular relaxation due to high stress in front of the crack tip, elastic deformation of molecules just prior to chain scisson (compare with theories for G_0 for materials in the rubbery state [2, 19]), and finally secondary crack systems. Heat generation is a problem by itself and is here regarded as a secondary effect.

Generally, models for cutting metals (in turning, milling or grinding) mainly describe the plastic shear deformation of the chips [30]. Doi and Yokoyama [31] present a theoretical model to predict cutting forces in wood. The only data needed were elastic properties and the friction coefficient, and the energy consuming mechanisms are elastic bending of the chip and the creation of two surfaces by a crack in front of the cutting edge. The model showed how to predict experimentally measured cutting forces in other brittle materials, such as unsaturated polyester and coal [32]. Cutting thickness was varied between 0.05 to 1.0 mm. However, it was impossible to fit the authors' data for W_S to the model. The level of modelled W_S was 3–10 times too low, even for a very high coefficient of friction. Furthermore, the model predict $W_S \to 0$ when $h \to 0$. This illustrates the need for better theoretical models.

One assumes that section bending, friction and the formation of subcrack systems are the major contributors to W_S at larger h. Work for molecular relaxation and elastic deformation of molecules prior to chain rupture are not believed to increase with increasing h. This is supported by the low energy values and chain scissions per square metre found in [2, 11, 16, 17]. In traditional (macroscopic) crack propagation tests, viscoelastic and plastic dissipation mechanisms are believed to be the main contributors to the measured fracture energy. The question then arises, is it possible for polymer molecules to do any extensive relaxation during sectioning? If the stress at the crack tip is assumed to approach zero at a certain distance in front of the crack tip, the time needed to develop fracture stresses would be 1/1000 s for a distance of 1 μm and a crack speed of 1 mm s^{-1}. This extremely short time is too short for any major molecular relaxation for the studied polymers at ambient temperature. However, the extent of the actual molecular relaxation remains unknown. Since it was seen that the dimensional changes were largest for the material with the steepest slope in Fig. 6, one suggests that the mechanism(s) responsible for increasing W_S with increasing h must also deform the section.

In order to evaluate fully the significance of every possible energy dissipation mechanism one needs to know more about the crack propagation process during sectioning. For instance, what is the rule of friction and how is the section compressed? The authors therefore need to develop the method further in order to measure F_t and F_r simultaneously. Furthermore, one needs to combine the force measurements with measurements of the dimensional changes, and finally analyse the damage from sectioning by transmission electron microscopy.

4. Conclusions

The sectioning forces during ultramicrotome sectioning were successfully measured by use of an instrumented sample holder. Sectioning forces as low as 5 mN could be measured. The work to section per unit area, W_S, was measured for sectioning thicknesses between 60 and 250 nm for five amorphous polymers

in the glassy state. W_S varied between 15 and 100 J m^{-2} depending on the material and section thickness, increasing W_S with increasing thickness. The differences between different polymers were found to be contradictory to macroscopic fracture toughness, G_{Ic} measurements. The material that showed the highest W_S had the lowest G_{Ic} values reported. The present results do not permit direct measurement of the intrinsic fracture energy, G_0. The major reason was the lack of minima in W_S.

References

1. A. J. KINLOCH and R. J. YOUNG, "Fracture Behaviour of Polymers" (Elsevier, London, 1988) p. 74.
2. N. E. KING and E. H. ANDREWS, *J. Mater. Sci.* **13** (1978) 1291.
3. L. H. SPERLING, "Introduction to Physical Polymer Science", 2nd Edn (Wiley, Toronto, 1992) p. 544.
4. J. BRANDRUP and E. H. IMMERGUT, "Polymer Handbook", 3rd Edn (Wiley, New York, 1989) pp. V78, V83, VI414–432.
5. H. H. KAUSCH, "Polymer Fracture" (Springer-Verlag, Berlin, 1987) p. 273.
6. D. C. PHILLIPS, J. M. SCOTT and M. JONES, *J. Mater. Sci.* **13** (1978) 311.
7. G. B. MCKENNA, J. M. CRISSMAN and A. LEE, *Polym. Prepr.* **29** (1988) 128.
8. H. F. MARK, N. M. BIKALES, C. G. OVERBERGER and G. MENGES (Eds), "Encylopedia of Polymer Science and Engineering" (Wiley, New York, 1987) p. 7.372.
9. L. ASP, L. A. BERGLUND and P. GUDMUNDSON, *Compos. Sci. Technol.* submitted.
10. R. J. MORGAN, F.-M. KONG and C. M. WALKUP, *Polymer* **25** (1984) 375.
11. G. J. LAKE and P. B. LINDLEY, *J. Appl. Polym. Sci.* **9** (1965) 1233.
12. R. J. MORGAN and J. E. O'NEAL, *Polym.-Plast. Technol. Eng.* **10** (1978) 49.
13. R. P. WOOL and A. T. ROCKHILL, *J. Macromol. Sci.-Phys.* **B20** (1981) 85.
14. K. A. MAZICH, M. A. SAMUS, C. A. SMITH and G. ROSSI, *Macromol.* **24** (1991) 2766.
15. A. G. ATKINS and J. F. V. VINCENT, *J. Mater. Sci. Lett.* **3** (1984) 310.
16. N. MOHAMMADI, R. BAGHERI, G. A. MILLER, A. KLEIN and L. H. SPERLNG, *Polym. Testing* **12** (1993) 65.
17. P. FORDYCE, B. M. FANCONI, and K. L. DEVRIES, *Polym. Eng. Sci.* **24** (1984) 421.
18. A. C.-M. YANG, C. K. LEE and S. L. FERLINE, *J. Polym. Sci. Polym. Phys. Ed.* **30** (1992) 1123.
19. G. J. LAKE and A. G. THOMAS, *Proc. R. Soc. Lond.* **A300** (1967) 108.
20. J. F. V. VINCENT, *Europ. Microsc. Anal.* May (1991) 13.
21. R. T. ALLISON and J. F. V. VINCENT, *J. Microsc.* **159** (1990) 203.
22. B. J. DOBRASZCZYK, A. G. ATKINS, G. JERONIMIDIS and P. P. PURSLOW, *Meat Sci.* **21** (1987) 25.
23. S. HODSON and J. MARSHALL, *J. Microsc.* **95** (1972) 459.
24. A. J. SAUBERMANN, W. D. RILEY and R. BEEUWKES III, *ibid.* **111** (1977) 39.
25. P. WIKEFELDT, PhD thesis, Chalmers Institute of Technology (1973) in Swedish.
26. H. F. HELANDER, *J. Microsc.* **101** (1974) 81.
27. J. L. WILLETT, K. M. O'CONNER and R. P. WOOOL, *J. Polym. Sci., Polym. Phys. Ed.* **24** (1986) 2583
28. W. J. PATZELT, "Polarisationsmikroskopie", Grundlagen, Instrumente, Anwendungen. Ernst Leitz GMBH (1974).
29. K. A. H. LINDBERG, PhD thesis 1987, Luleå University of Technology (1987).
30. R. M. D. MESQUITA and M. J. M. BARATA MARQUES, *J. Mater. Process. Technol.* **33** (1992) 229.
31. O. DOI and M. YOKOYAMA, *Bull. JSME* **18** (1975) 905.
32. *Idem. ibid.* **21** (1978) 161.

Received 23 September 1994
and accepted 28 April 1995